Functionalized Mesoporous Films

DOI: 10.1002/ange.201309447

Electrochemically Assisted Generation of Highly Ordered Azide-Functionalized Mesoporous Silica for Oriented Hybrid Films**

*Neus Vilà, Jaafar Ghanbaja, Emmanuel Aubert, and Alain Walcarius**

Abstract: *One key challenge in inorganic mesoporous films is the development of oriented mesostructures with vertical channels, and even more challenging is their functionalization while maintaining accessible the selected surface groups. Combining the electrochemically assisted deposition of ordered and oriented azide-functionalized mesoporous silica with alkyne–azide click chemistry enables such nanostructured and vertically aligned hybrid films to be obtained with significant amounts of active organic functional groups, as illustrated for ferrocene and pyridine functions. A good level of mesostructural order was obtained, namely up to 40 % of organosilane in the starting sol. The method could be applied to a wide variety of functional groups, thus offering numerous new opportunities for applications in various fields.*

Supramolecular templating methods have revolutionized the synthesis of high-surface-area materials with uniform and large pores arranged in well-defined mesostructures. Bottom-up self-assembly of sol–gel networks around surfactant templates[1] provides a unique method to prepare a wide range of mesostructured solids with unprecedented properties in terms of porosity, structure, and reactivity,[2] with promising applications in various fields.[3] They can be obtained with various morphologies,[4] but thin films have proven to be the most suitable configuration in many cases.[3g,4a,5] Apart from a few examples of unsupported membranes,[6] mesoporous silica films have been prepared on solid supports,[4a,7] most often by evaporation-induced self-assembly (EISA).[8]

For practical applications, it is essential to ensure accessible mesopores from surfaces with fast mass transport through the film,[9] but the morphological control of surfactant-templated films has proven to be very difficult by EISA,[10] tending to favor the parallel orientation of mesochannels.[11] To overcome this limitation, some strategies to generate vertically aligned mesoporous silica films have recently appeared: confinement and self-assembly in exo-templates (pre-assembled block copolymers[12] or porous membranes);[13] use of patterned supports, surface alignment by π–π interactions, or combination of photoaligning and micropatterning;[14] epitaxial growth;[15] magnetically induced orientation;[16] electro-assisted self-assembly;[17] or Stöber-solution growth.[18] Most approaches were restricted to large mesopores (more than 5–6 nm in diameter),[14b,17,18] and many of them have significant drawbacks (sophisticated processes, time-consuming and complex substrate pre-treatments, low level of pore orientation, restricted choice of support type or geometry). More dramatically, they have been mostly applied to non-functionalized thin films (that is, an inherent limitation for practical applications).

Still challenging is thus the development of a simple and general route to built-in functional sites in mesoporous silica films. To date, only the electro-assisted deposition method has been applied to the self-assembly cocondensation of alkoxysilane and organosilane to grow functionalized and vertically aligned mesochannels, but this was restricted to very simple organic functional groups (that is, methyl, amine, thiol),[19] whereas attempts made with more sophisticated organosilanes (for example, bearing ferrocene or cyclam derivatives) failed owing to lack of mesostructuration/orientation or phase separation.[20] Basically, post-grafting could be applied, but it led to dramatic blocking effects when applied to small mesopore channels oriented normal to the support (Supporting Information, Section S1).

Herein, we present an unprecedented, universal, and simple approach combining electro-assisted self-assembly (EASA) and click chemistry to generate functionalized, highly ordered, and vertically oriented mesoporous thin films. Although the azide–alkyne click chemistry approach has been exploited previously to functionalize mesoporous silica using (3-azidopropyl)trimethoxysilane (AzPTMS) as the organoazide source, it was almost exclusively restricted to large pore SBA-15 powders,[21] at the exception of one example of small pore mesoporous silica particles[22] and another one of silica microdot arrays,[23] all of them being limited to a maximum of 10 mol % AzPTMS in the material. The method proposed here is not only likely to generate clickable, vertically aligned mesopores ordered over wide areas, but also to get a high functionalization level (up to 40 mol % AzPTMS in the starting sol) with azide groups likely to react with a variety of organic molecules possessing an alkyne terminal group (as illustrated using ethynylferrocene or ethynylpyridine).

The synthesis (Scheme 1) involves the use of a hydro-alcoholic sol containing tetraethoxysilane (TEOS) and

[*] Dr. N. Vilà, Dr. A. Walcarius
Laboratoire de Chimie Physique et Microbiologie pour l'Environnement, UMR 7564, CNRS-Université de Lorraine
405 rue de Vandoeuvre, 54600 Villers-les-Nancy (France)
E-mail: alain.walcarius@univ-lorraine.fr
Dr. J. Ghanbaja
Institut Jean Lamour, UMR 7198, CNRS-Université de Lorraine (France)
Dr. E. Aubert
Cristallographie, Résonance Magnétique et Modélisations, UMR 7036, CNRS-Université de Lorraine (France)

[**] We thank Dr. F. Quilès for IR spectroscopy, A. Renard for XPS, Dr. T. Rozhanchuk for permeability measurements after grafting, and Dr. M. Etienne for helpful discussions.

Supporting information for this article is available on the WWW under http://dx.doi.org/10.1002/anie.201309447.

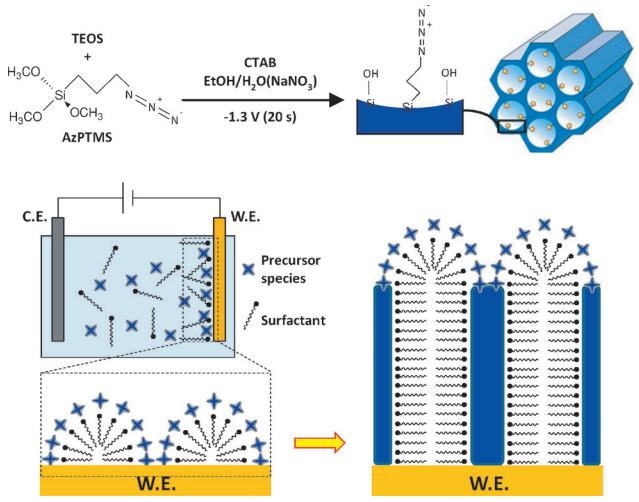

Scheme 1. Illustration of the EASA co-condensation process of AzPTMS and TEOS in the presence of CTAB to get vertically aligned azide-functionalized mesoporous silica film (W.E. = working electrode; C.E. = counter electrode).

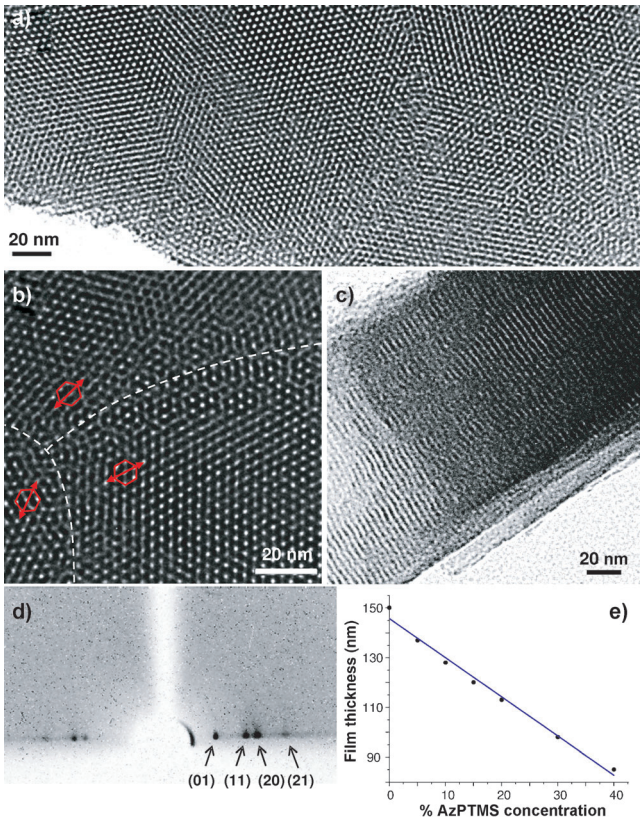

Figure 1. TEM micrographs of an electrogenerated mesoporous silica thin film incorporating azide groups obtained from a sol prepared with 20 mol% AzPTMS and 80 mol% TEOS precursor contents ($C_{(TEOS+AzPTMS)}$ = 200 mM); a) top view; b) magnified top view TEM micrographs; c) cross-section view; d) GIXRD pattern; e) variation of the film thickness as a function of the% AzPTMS.

AzPTMS[24] in selected ratios (from 99:1 to 60:40), cetyltrimethylammonium bromide (CTAB) as template, and $NaNO_3$ as electrolyte, in which the electrode (ITO, indium–tin oxide) was immersed and a cathodic potential of −1.3 V was applied for 20 s (optimized values) to induce self-assembly co-condensation of the precursors and the template. More experimental details can be found in the Supporting Information, Section 2. The applied potential not only plays the role of generating the hydroxyl catalysts likely to accelerate the condensation process,[25] but it also contributes to pre-assemble transient CTAB hemi-micelles on the electrode surface,[26] thereby inducing the generation of ordered, hexagonally packed, and orthogonally oriented mesopore channels (Figure 1 a–c). Consistent with previous observations made on pure siliceous materials,[17] the azide-functionalized thin films kept their mesostructural order over wide areas (Supporting Information, Figure S4) with grain boundaries between hexagonal regions (Figure 1 b). Grazing incidence X-ray diffraction (GIXRD) was been used to further confirm the perpendicular orientation of all meso-channels. The GIXRD pattern (see Figure 1 d for 20% AzPTMS sample) exhibits typical spots of a vertically oriented hexagonal mesostructure,[17b,19b] without any out-of-plane refection, indicating a high level of ordering and orientation over the whole surface area. From the position of GIXRD spots associated to the 10, 11, 20, and 21 reflections of hexagonal symmetry of the *p6mm* space group, a *d* spacing of 4.1 nm can be determined, which corresponds well to the center-to-center distance between two adjacent mesopores, as roughly estimated from TEM images (3.9 nm). More overwhelming is that mesostructuration and vertical alignment are kept over a wide composition range, up to 40 mol% of AzPTMS in the sol (Supporting Information, Figure S5), which could be due to favorable electrostatic interactions between zwitterionic AzPTMS with both the positively charged surfactant and negatively charged silica surface. Independently, on the azide group content, the *d* spacing remained constant (that is, 4.0–4.1 nm), and it could be slightly adjusted around this value by varying the alkyl chain length of the surfactant.[17b] On the other hand, the functionalization level affected the film thickness, resulting in a progressive decrease when increasing the amount of azide groups (Figure 1 e). Such effect is attributed to slower polycondensation of the organosilane precursor in comparison to TEOS, as already reported for methyl functionalized films.[19b]

The presence of the azide-terminated groups covalently bonded to the mesoporous silica film is supported by IR spectroscopy, by the strong asymmetric band observed at 2095 cm^{-1} (attributed to the N_3 groups)[27] increasing proportionally to the functionalization level (Supporting Information, Figure S6). Another yet indirect way to evidence the successful incorporation of azide groups in the material is the characterization of the film permeability. This can be achieved by cyclic voltammetry using a redox probe ($[Ru(NH_3)_6]^{3+}$ in this case) in solution (Figure 2). Focusing first on the 5:95 AzPTMS/TEOS film (Figure 2 a), the absence of any signal prior to surfactant extraction can clearly be seen, indicating the presence of a crack-free film over the whole electrode surface. After surfactant removal, the azide-functionalized film was highly porous as the voltammetric signals were of the same order of magnitude as that recorded using the bare ITO electrode. A similar trend was observed using

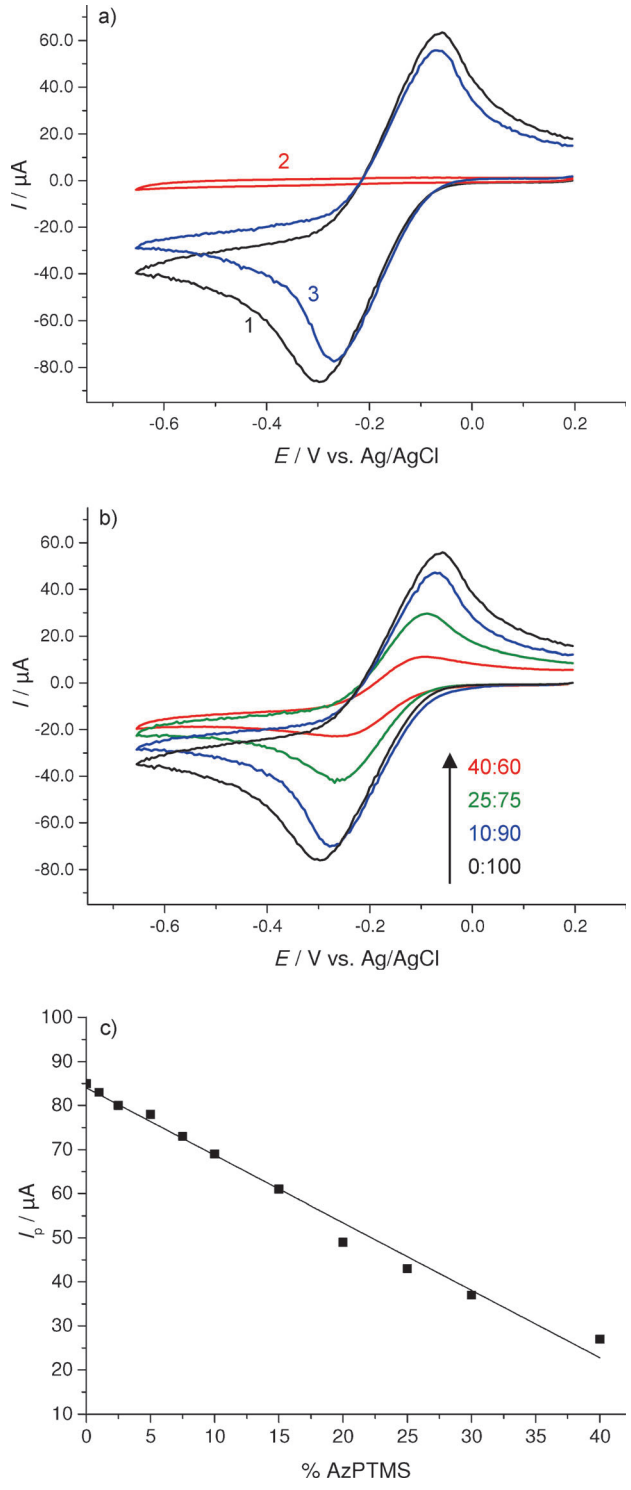

Figure 2. Cyclic voltammograms recorded in 1 mM $[Ru(NH_3)_6]^{3+}$ aqueous solution (0.1 M $NaNO_3$) using a) ITO bare electrode (1), ITO electrode covered with an azide-functionalized silica film (AzPTMS/TEOS: 5:95) before (2) and after (3) surfactant removal; b) ITO electrode covered with azide-functionalized silica films after surfactant removal for various AzPTMS/TEOS ratios: 0:100 (black line), 5:95 (blue line), 20:80 (green line), 40:60 (red line); c) variation of peak currents as a function of the amount of azide groups. Scan rate: 20 $mV s^{-1}$.

ferrocenediethanol as redox probe, demonstrating also the successful complete removal of the surfactant template (Supporting Information, Figure S7). Increasing the azide loading in the film then resulted in a continuous decrease in the voltammetric signals (Figure 2b,c), which was due to stronger resistance to mass transport as a result of the progressive filling of the pores. The linear variation supports an incorporation of azide groups proportionally to the AzPTMS/TEOS ratio in the sol, as also supported by XPS data, indicating 70–75% azide incorporation yields (Supporting Information, Figure S8).

The Huisgen (click) reaction carried out under mild conditions would allow the coupling of azide terminal groups located in such vertically aligned mesoporous silica films with a variety of organic molecules possessing an alkyne group in their structure. To illustrate the feasibility of this reaction in the confined space of mesopore channels, and to point out the versatility of the approach, several molecules with such structural conditions have been chosen (ethynylferrocene, propargyl alcohol, 3-ethynylthiophene, and 2-ethynylpyridine). The interest of ferrocene is its electrochemical activity (a straightforward way to demonstrate successful functionalization), while the others should be more readily characterized by IR or UV/Vis spectroscopy to evidence the derivatization process contrary to the ethynylferrocene, which presents a characteristic band located in the same spectral region as the 1,2,3-triazole rings.

The successful ferrocene grafting (for experimental details, see the Supporting Information, Section S2) is demonstrated through the well-defined voltammetric curves that have been obtained in both organic medium (acetonitrile + 0.1 M $TBAClO_4$; Figure 3a)) and in aqueous solution (0.1 M $NaNO_3$; Figure 3b,c). The electrochemical response grows as a function of the azide loading in the film prepared from AzPTMS/TEOS ratios in the range 2.5:97.5 to 40:60 (Figure 3a, inset), confirming the good accessibility of azide groups for the click reaction to take place. Even if it was not possible to determine the exact composition of the hybrid films (too low amount of material to enable elemental analysis), these results suggest however that the amount of ethynylferrocene coupling with the azide-functionalized film increases when larger amounts of AzPTMS was employed to synthesize the starting film. Both the shape of the voltammograms and the linear variation of peak currents with the scan rates in the range of 5–80 $mV s^{-1}$ (Figure 3b, inset) are typical of a surface-controlled charge transfer process.[28] From the integration of peak currents, one can estimate a content of 3×10^{-5} $mol g^{-1}$ ferrocene in the film. The mechanism of electron transfer should be the electron hopping between adjacent ferrocene centers, as the direct electron transfer is not possible owing to the insulating character of the silica walls and diffusion of ferrocene moieties is impeded by their covalent bonding to the silica material. This is also supported by no noticeable voltammetric signal for the ferrocene-functionalized films prepared from AzPTMS/TEOS ratios lower than 2.5:97.5, as a result of too low amount of ferrocene groups (located too far from each other to enable electron hopping). Interestingly, continuous potential cycling led to nearly stable voltammetric signals in aqueous medium (Fig-

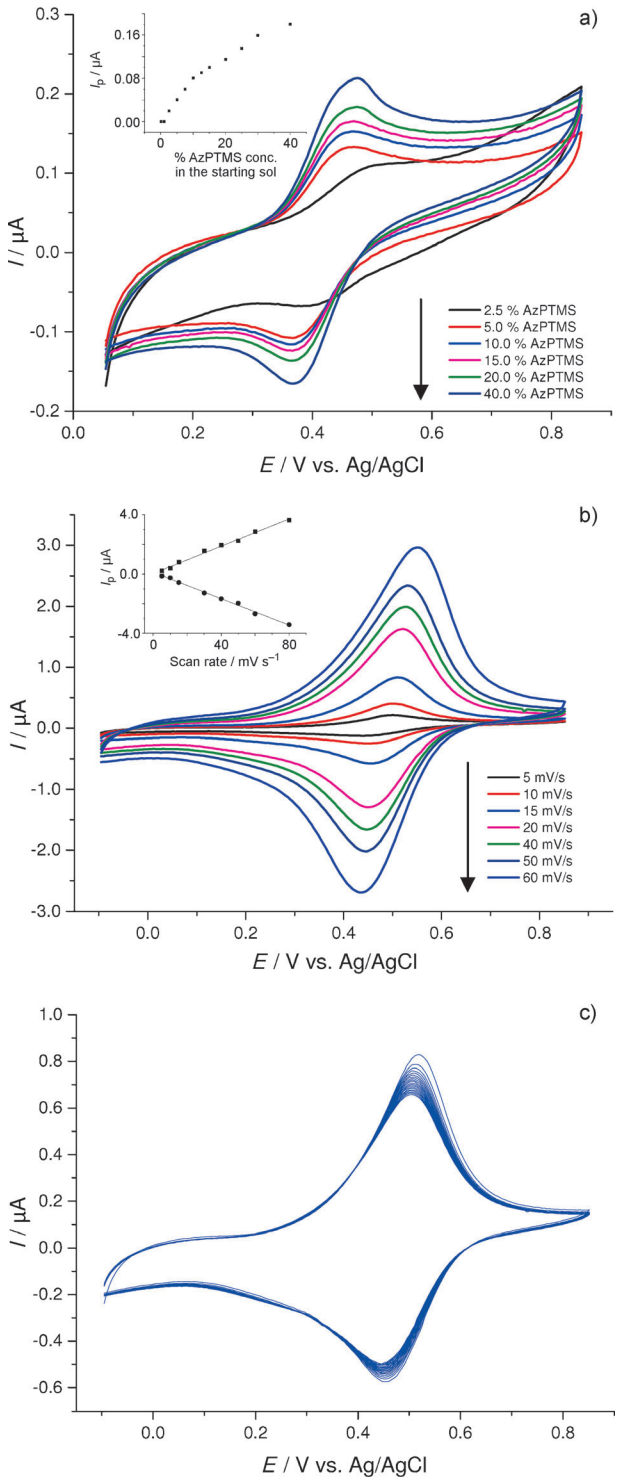

Figure 3. Cyclic voltammograms recorded using ITO electrodes covered with a ferrocene-functionalized silica film in a) acetonitrile (+0.1 M $TBAClO_4$) for films prepared from various AzPTMS/TEOS ratios (100 mM total concentration) at 20 mV s^{-1}; b), c) aqueous solution (0.1 M $NaNO_3$) for a film prepared from 40:60 AzPTMS/TEOS ratio (200 mM total concentration) at various potential scan rates (b) or at 20 mV s^{-1} for 20 successive cycles (c). Insets: in (a): the variation of anodic peak currents as a function of% AzPTMS; in (b): the variation of anodic and cathodic peak currents as a function of potential scan rate.

ure 3c), indicating durable immobilization of ferrocene in an electroactive form, contrary to other related systems,[29] and the long-term stability was even better in organic media (Supporting Information, Figure S9). Even more overwhelming is that the ferrocene-functionalized films remained permeable to external reagents, as pointed out by cyclic voltammetry using $[Ru(NH_3)_6]^{3+}$ as a redox probe (Figure 4).

The transformation of azide moieties to 1,2,3-triazole cores has been followed by IR spectroscopy, by the attenu-

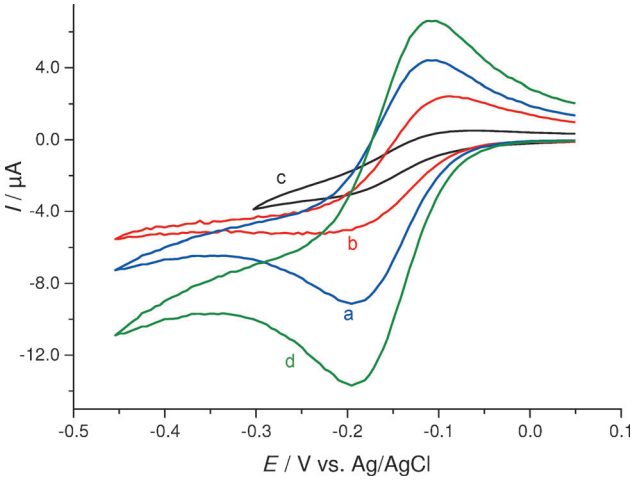

Figure 4. Cyclic voltammograms recorded in 1 mM $[Ru(NH_3)_6]^{3+}$ (+0.1 M $NaNO_3$) using ITO electrodes covered with ferrocene-functionalized silica films prepared from various AzPTMS/TEOS ratios: 10–90 (a), 20–80 (b), 40–60 (c); the curve obtained on bare ITO (d) is also shown.

ation of the strong asymmetric stretching absorption band of the azide centered at 2095 cm^{-1} (Supporting Information, Figure S10). Total disappearance of this band was indeed observed for the films containing less that 30% azide groups, whereas higher contents led to a residual signal observed in the IR spectra, suggesting the presence of some unreacted N_3 functions. On the other hand, the formation of 1,2,3-triazole rings from the azide-functionalized film was evidenced by the emergence of a broad and intense characteristic absorption band at 1610 cm^{-1} when performing the click reaction with propargyl alcohol instead of ethynylferrocene as a coupling reagent, consistent with literature data.[30] XPS further confirms the effectiveness of the Huisgen reaction (Supporting Information, Figure S11), by the transformation of the N1s signal characteristic of the N_3 group (specific azide component centered at 405.0 eV)[31] into that related to the 1,2,3-triazole function (bands at 402.3 and 400.1 eV).[32]

To highlight the versatility of the method, the azide-functionalized films were derivatized with 3-ethynylthiophene and 2-ethynylpyridine; these reactions were followed by UV/Vis spectroscopy. In all cases, the reaction was successful and an illustration based on the pyridine derivative is given on Figure 5. The possibility to afford mesoporous films bearing pyridine groups is indeed attractive as it would allow the coordination of organometallic complexes, such as $[Fe(bpy)_2Cl_2]$. Preliminary results have been obtained, evi-

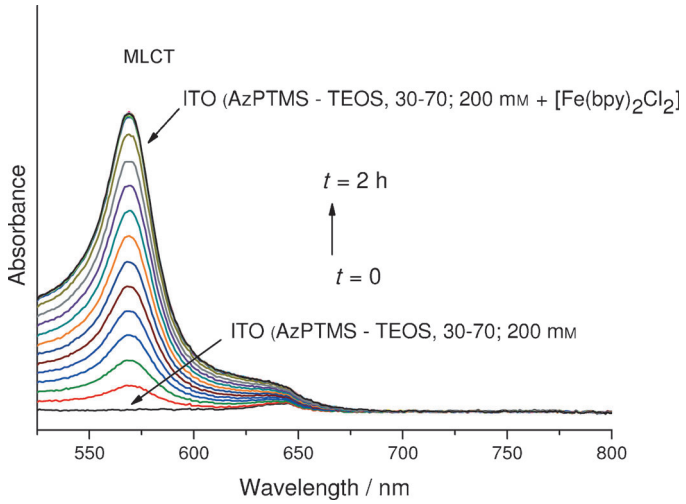

Figure 5. Evolution of the UV/Vis spectra of a film prepared from a sol containing AzPTMS-TEOS (30–70; $c = 200$ mM) upon reaction with ethynylpyridine and subsequent coordination of $[Fe(bpy)_2Cl_2]$.

dencing the feasibility of such approach. The pyridine-functionalized films were dipped into a solution containing 1 mM $[Fe(bpy)_2Cl_2]$ in acetonitrile and series of UV/Vis spectra were recorded every five minutes (Figure 5). The coordination of the iron complex to the pyridine groups was evidenced by the appearance of a metal-to-ligand charge transfer (MLCT) absorption band at 570 nm, in good agreement with data obtained in solution displaying a sharper absorption band located at 560 nm. No more evolution of the absorption band was observed after 2 h when a maximum of the absorbance value was reached.

In summary, a versatile method based on the combination of an azide–alkyne click chemistry approach with electro-assisted self-assembly has been developed to functionalize highly ordered and vertically aligned mesoporous silica films under mild conditions. Such electrogenerated thin films kept their ordered and oriented mesostructure up to 40% of organosilane in the starting sol. Further derivatization of the mesoporous material can be readily afforded based on a Huisgen click reaction between the easily accessible azide groups and alkyne derivatives. The method can be basically extended to a variety of functional groups, thus offering numerous new opportunities for applications in various fields.

Received: October 30, 2013
Revised: January 7, 2014
Published online: February 12, 2014

Keywords: click chemistry · electrochemistry · mesoporous materials · silica films · vertical mesopore channels

[1] a) C. T. Kresge, M. E. Leonowicz, W. J. Roth, J. C. Vartuli, J. S. Beck, *Nature* **1992**, *359*, 710–712; b) D. Zhao, J. Feng, Q. Huo, N. Melosh, G. H. Fredrickson, B. F. Chmelka, G. D. Stucky, *Science* **1998**, *279*, 548–552.

[2] a) F. Hoffmann, M. Cornelius, J. Morell, M. Froeba, *Angew. Chem.* **2006**, *118*, 3290–3328; *Angew. Chem. Int. Ed.* **2006**, *45*, 3216–3251; b) Y. Wan, D. Zhao, *Chem. Rev.* **2007**, *107*, 2821–2860.

[3] a) J. L. Vivero-Escoto, B. G. Trewyn, V. S.-Y. Lin, *Annu. Rev. Nano Res.* **2009**, *3*, 191–231; b) A. Walcarius, L. Mercier, *J. Mater. Chem.* **2010**, *20*, 4478–4511; c) M. Vallet-Regí, M. Colilla, B. González, *Chem. Soc. Rev.* **2011**, *40*, 596–607; d) T. Lebold, J. Michaelis, C. Braeuchle, *Phys. Chem. Chem. Phys.* **2011**, *13*, 5017–5033; e) Z. Zhou, M. Hartmann, *Chem. Soc. Rev.* **2013**, *42*, 3894–3912; f) U. Díaz, D. Brunel, A. Corma, *Chem. Soc. Rev.* **2013**, *42*, 4083–4097; g) A. Walcarius, *Chem. Soc. Rev.* **2013**, *42*, 4098–4140.

[4] a) C. Sanchez, C. Boissière, D. Grosso, C. Laberty, L. Nicole, *Chem. Mater.* **2008**, *20*, 682–737; b) J. Li, J. Liu, D. Wang, R. Guo, X. Li, W. Qi, *Langmuir* **2010**, *26*, 12267–12272; c) C. Mao, F. Wang, B. Cao, *Angew. Chem.* **2012**, *124*, 6517–6521; *Angew. Chem. Int. Ed.* **2012**, *51*, 6411–6415; d) S.-H. Wu, C.-Y. Mou, H.-P. Lin, *Chem. Soc. Rev.* **2013**, *42*, 3862–3875; e) K. Shiba, N. Shimura, M. Ogawa, *J. Nanosci. Nanotechnol.* **2013**, *13*, 2483–2494.

[5] P. Innocenzi, L. Malfatti, *Chem. Soc. Rev.* **2013**, *42*, 4198–4216.

[6] a) S. Schacht, Q. Huo, I. G. Voigt-Martin, G. D. Stucky, F. Schüth, *Science* **1996**, *273*, 768–771; b) L. Faget, A. Berman, O. Regev, *Thin Solid Films* **2001**, *386*, 6–13; c) H. Yang, N. Coombs, I. Sokolov, G. A. Ozin, *Nature* **1996**, *381*, 589–592; d) K. J. Edler, B. Yang, *Chem. Soc. Rev.* **2013**, *42*, 3765–3776.

[7] a) Y. Lu, R. Ganguli, C. A. Drewien, M. T. Anderson, C. J. Brinker, W. Gong, Y. Guo, H. Soyez, B. Dunn, M. H. Huang, J. I. Zink, *Nature* **1997**, *389*, 364–368; b) M. Ogawa, *Curr. Top. Colloid Interface Sci.* **2001**, *4*, 209–217.

[8] a) C. J. Brinker, Y. Lu, A. Sellinger, H. Fan, *Adv. Mater.* **1999**, *11*, 579–585; b) D. Grosso, F. Cagnol, G. J. D. A. A. Soler-Illia, E. L. Crepaldi, H. Amenitsch, A. Brunet-Bruneau, A. Bourgeois, C. Sanchez, *Adv. Mater.* **2004**, *16*, 309–322.

[9] a) U.-H. Lee, M.-H. Kim, Y.-U. Kwon, *Bull. Korean Chem. Soc.* **2006**, *27*, 808–816; b) M. Etienne, A. Quach, D. Grosso, L. Nicole, C. Sanchez, A. Walcarius, *Chem. Mater.* **2007**, *19*, 844–856; c) M. Etienne, Y. Guillemin, D. Grosso, A. Walcarius, *Anal. Bioanal. Chem.* **2013**, *405*, 1497–1512.

[10] C. J. Brinker, D. R. Dunphy, *Curr. Opin. Colloid Interface Sci.* **2006**, *11*, 126–132.

[11] a) H. Yang, A. Kuperman, N. Coombs, S. Mamiche-Afara, G. A. Ozin, *Nature* **1996**, *379*, 703–705; b) L. Nicole, C. Boissière, D. Grosso, A. Quach, C. Sanchez, *J. Mater. Chem.* **2005**, *15*, 3598–3627; c) M. P. Tate, B. W. Eggiman, J. D. Kowalski, H. W. Hillhouse, *Langmuir* **2005**, *21*, 10112–10118.

[12] a) V. R. Koganti, S. E. Rankin, *J. Phys. Chem. B* **2005**, *109*, 3279–3283; b) E. M. Freer, L. E. Krupp, W. D. Hinsberg, P. M. Rice, J. L. Hedrick, J. N. Cha, R. D. Miller, H.-C. Kim, *Nano Lett.* **2005**, *5*, 2014–2018; c) B. W. Eggiman, M. P. Tate, H. W. Hillhouse, *Chem. Mater.* **2006**, *18*, 723–730; d) S. Nagarajan, M. Li, R. A. Pai, J. K. Bosworth, P. Busch, D.-M. Smilgies, C. K. Ober, T. P. Russel, J. J. Watkins, *Adv. Mater.* **2008**, *20*, 246–251.

[13] a) A. Yamaguchi, F. Uejo, T. Yoda, T. Uchida, Y. Tanamura, T. Yamashita, N. Teramae, *Nat. Mater.* **2004**, *3*, 337–341; b) Q. Lu, F. Gao, S. Komarneni, T. E. Mallouk, *J. Am. Chem. Soc.* **2004**, *126*, 8650–8651; c) B. Platschek, R. Koehn, M. Doeblinger, T. Bein, *ChemPhysChem* **2008**, *9*, 2059–2067; d) R. A. Farrell, N. Petkov, M. A. Morris, J. D. Holmes, *J. Colloid Interface Sci.* **2010**, *349*, 449–472.

[14] a) H. Fukumoto, S. Nagano, N. Kawatsuki, T. Seki, *Chem. Mater.* **2006**, *18*, 1226–1234; b) M. Hara, S. Nagano, T. Seki, *J. Am. Chem. Soc.* **2010**, *132*, 13654–13656.

[15] a) H. Miyata, *Microporous Mesoporous Mater.* **2007**, *101*, 296–302; b) E. K. Richman, T. Brezesinski, S. H. Tolbert, *Nat. Mater.* **2008**, *7*, 712–717.

[16] Y. Yamauchi, M. Sawada, M. Komatsu, A. Sugiyama, T. Osaka, N. Hirota, Y. Sakka, K. Kuroda, *Chem. Asian J.* **2007**, *2*, 1505 – 1512.
[17] a) A. Walcarius, E. Sibottier, M. Etienne, J. Ghanbaja, *Nat. Mater.* **2007**, *6*, 602 – 608; b) A. Goux, M. Etienne, E. Aubert, C. Lecomte, J. Ghanbaja, A. Walcarius, *Chem. Mater.* **2009**, *21*, 731 – 741.
[18] Z. Teng, G. Zheng, Y. Dou, W. Li, C.-Y. Mou, X. Zhang, A. M. Asiri, D. Zhao, *Angew. Chem.* **2012**, *124*, 2215 – 2219; *Angew. Chem. Int. Ed.* **2012**, *51*, 2173 – 2177.
[19] a) M. Etienne, A. Goux, E. Sibottier, A. Walcarius, *J. Nanosci. Nanotechnol.* **2009**, *9*, 2398 – 2406; b) Y. Guillemin, M. Etienne, E. Aubert, A. Walcarius, *J. Mater. Chem.* **2010**, *20*, 6799 – 6807; c) G. Herzog, E. Sibottier, M. Etienne, A. Walcarius, *Faraday Discuss.* **2013**, *164*, 259 – 273.
[20] Unpublished results.
[21] a) J. Nakazawa, T. D. P. Stack, *J. Am. Chem. Soc.* **2008**, *130*, 14360 – 14361; b) B. Malvi, B. R. Sarkar, D. Pati, R. Mathew, T. G. Ajithkumar, S. Sen Gupta, *J. Mater. Chem.* **2009**, *19*, 1409 – 1416; c) J. Nakazawa, B. J. Smith, T. D. P. Stack, *J. Am. Chem. Soc.* **2012**, *134*, 2750 – 2759.
[22] N. Moitra, P. Trens, L. Raehm, J.-O. Durand, X. Cattoën, M. Wong Chi Man, *New J. Chem.* **2011**, *35*, 13476 – 13482.
[23] O. De Los Cobos, B. Fousseret, M. Lejeune, F. Rossignol, M. Duteilh-Colas, C. Carrion, C. Boissière, F. Ribot, C. Sanchez, X. Cattoën, M. Wong Chi Man, J.-O. Durand, *Chem. Mater.* **2012**, *24*, 4337 – 4342.
[24] a) G. Righi, C. D'Achille, G. Pescatore, C. Bonini, *Tetrahedron Lett.* **2003**, *44*, 6999 – 7002; b) N. Halland, A. Braunton, S. Bachmann, M. Marigo, K. A. Jørgensen, *J. Am. Chem. Soc.* **2004**, *126*, 4790 – 4791; c) G. P. Miller, E. T. Kool, *J. Org. Chem.* **2004**, *69*, 2404 – 2410.
[25] a) K.-S. Choi, E. W. McFarland, G. D. Stucky, *Adv. Mater.* **2003**, *15*, 2018 – 2021; b) M. Chen, I. Burgess, J. Lipkowski, *Surf. Sci.* **2009**, *603*, 1878 – 1891.
[26] a) R. Shacham, D. Avnir, D. Mandler, *Adv. Mater.* **1999**, *11*, 384 – 388; b) E. Sibottier, S. Sayen, F. Gaboriaud, A. Walcarius, *Langmuir* **2006**, *22*, 8366 – 8373; c) M. M. Collinson, *Acc. Chem. Res.* **2007**, *40*, 777 – 783.
[27] C. N. Ramachandra, T. S. Chao, C. W. W. Hoffman, *Anal. Chem.* **1957**, *29*, 916 – 918.
[28] E. Laviron, *J. Electroanal. Chem.* **1979**, *100*, 263 – 270.
[29] C. Delacôte, J.-P. Bouillon, A. Walcarius, *Electrochim. Acta* **2006**, *51*, 6373 – 6383.
[30] E. Borello, A. Zecchina, E. Guglielminotti, *J. Chem. Soc. B* **1966**, 1243 – 1245.
[31] a) E. W. Wollman, D. Kang, C. D. Frisbie, I. M. Lorkovic, M. S. Wrighton, *J. Am. Chem. Soc.* **1994**, *116*, 4395 – 4404; b) J. P. Collman, N. K. Devaraj, T. P. A. Eberspacher, C. E. D. Chidsey, *Langmuir* **2006**, *22*, 2457 – 2464.
[32] S. Ciampi, T. Böcking, K. A. Kilian, M. James, J. B. Harper, J. Gooding, *Langmuir* **2007**, *23*, 9320 – 9329.

